CHAPTER III

Antiferromagnetic interactions through phenoxo-bridges and lattice water. Synthesis, structure and magnetic properties of new Mn(III) Schiff base complexes in combination with thiocyanate ligand

3.1. Introduction

The five coordinate Mn^{3+} ion in Mn(SB)X, where SB is a tetradentate Schiff base[1] and X is a halide or pseudohalide, is known to attain six coordination in certain cases through the formation of a X-bridged one-dimensional chain or a phenoxo-bridged dimer.[2] There are also cases where the sixth coordination position is occupied by a solvent molecule, usually water.[3] In the case of phenoxo-bridged dimers, depending upon the Mn···O bond-length and Mn-O···Mn bond-angle, these complexes may show an intra-dimer ferro or antiferromagnetic interaction.[4-16] Dinuclear as well as larger assemblies formed by Mn(III) with tetradentate Schiff base ligands have been recently reviewed.[17] In the present work we report on two complexes, Mn(acphen)NCS and Mn(acphpn)(H_2O)NCS, where the ligands acphen and acphpn are obtained *in situ* by condensing 2-hydroxyacetophenone with 1,2-diaminoethane and 1,3-diaminopropane, respectively. The complex of acphen is a phenoxo-bridged dimer while the acphpn ligand yields a mononuclear aquo complex as a dihydrate. A previous preparation[3] using acphenH_2 had resulted in a mononuclear complex, Mn(acphen)(H_2O)NCS, even for acphen. An important result

from the present study is that both the compounds show weak antiferromagnetic coupling between Mn(III) centres. In the case of the mononuclear acphpn complex, the interaction arises from the presence of lattice water molecules, in sharp contrast to the above mentioned complex of acphen which forms only anhydrous crystals and displays no significant magnetic interaction.

3.2. Experimental Section

3.2.1. Synthesis

2-Hydroxyacetophenone, 1,2-diaminoethane and 1,3-diaminopropane were of reagent grade. The Schiff bases were formed *in situ* in the presence of the appropriate metal salt. Perchlorate salts are potentially explosive and should be prepared only in small quantities and handled with care.

$[Mn(acphen)NCS]_2$ (1): In a beaker open to the atmosphere, $Mn(CH_3COO)_2.4H_2O$ (0.245g, 1.00 mmol) and KSCN (0.194g, 2.00 mmol) were stirred in methanol (25 mL). 2-Hydroxyacetophenone(0.272g, 2.00 mmol) and 1,2-diaminoethane (0.060g, 1.0 mmol) were stirred in methanol (30 mL) and added to the above solution; stirring was continued for about 2h to complete the aerial oxidation of Mn^{2+} to Mn^{3+}. The filtered solution kept in a refrigerator (5 °C) yielded dark green crystals after 3 days. Yield: 0.252g (0.31 mmol, 62%). Anal. Cald. for $Mn_2C_{38}H_{36}N_8O_4S_2$: C, 56.02; H, 4.45; N, 10.31. Found: C, 56.18; H, 4.45; N, 10.78. Significant IR absorptions (cm^{-1}): 2054, 1599, 1535, 1433, 1325, 1140, 1084, 856, 750, 472.

$[Mn(acphpn)(H_2O)NCS]\cdot 2H_2O$ (2): In a beaker open to the atmosphere, 2-hydroxyacetophenone (0.272 g, 2.00 mmol) and 1,3-diaminopropane (0.071g 1.0

mmol) were stirred in methanol (40mL). $Mn(ClO_4)_2.6H_2O$ (0.361g, 1.00 mmol) was added, and the stirring was continued for about 1h. To the resulting solution, KSCN (0.194g, 2.00 mmol) dissolved in water (10 mL) was added, stirred for 5 minutes, and the filtered solution kept aside at room temperature for one day, over which time dark green crystals deposited. Yield: 0.289g (0.607 mmol, 60.7%). Anal. Calcd. for $MnC_{20}H_{26}N_3O_5S$: C, 50.53; H, 5.51; N, 8.84. Found: C, 50.48; H, 5.50; N, 9.03. Significant IR absorptions (cm^{-1}): 3344, 3200, 2085, 1643, 1597, 1433, 1319, 1150, 937, 854, 760, 599, 464.

3.2.2. Physical measurements

IR spectra were obtained in KBr pellets using Shimadzu FT-IR 8000 spectrometer. Elemental analysis of the complexes was performed on a FLASH EA SERIES CHNS analyzer. Absorption spectra for **1** and **2** in methanol were recorded on a Shimadzu UV-3100 PC spectrometer. The magnetic susceptibility was measured for **1** and **2** in a magnetic field of 5000 Oe and in the temperature range 1.98-300 K using a Quantum Design MPMS SQUID susceptometer. The samples were pressed into pellets to avoid orientation effects of the microcrystals during magnetic measurements. Diamagnetic corrections were applied using Pascal's constants. Fitting of the susceptibility data was initially done by using the program SUSCEP[18] based on the dimer equation[19a] for **1** and Curie-Weiss equation as well as chain equation[19b] for **2**. Final fittings for **1** were carried out through exact diagonalisation of the energy matrix including an axial zero field splitting (zfs) term,

Table 3.1. Crystallographic data and structure refinement for **1** and **2**

	1	**2**
Formula	$C_{38}H_{36}Mn_2N_6O_4S_2$	$C_{20}H_{26}MnN_3O_5S$
Formula weight	814.75	475.44
Crystal system	triclinic	orthorhombic
a (Å)	7.9128(6)	9.3234(8)
b (Å)	9.9970(7)	14.2756(12)
c (Å)	11.1144(8)	16.1270(14)
α (º)	92.7200(10)	90
β (º)	90.2690(10)	90
γ (º)	91.5390(10)	90
V (Å^3)	877.87(11)	2146.5(3)
Space group	$P\bar{1}$	*Pnma*
Z	1	4
T (K)	100(2)	100(2)
ρ_{calcd} (g cm^{-3})	1.541	1.471
μ (mm^{-1})	0.890	0.749
θ Range (º)	1.83 - 28.27	1.91 - 28.21
h/k/l indices	-10, 10/ -12, 13/ -14, 14	-12, 12/ -18, 18/ -21, 21
Reflections collected	10292	23625
Unique reflection, R_{int}	4094, 0.0367	2667, 0.0263
GooF	1.121	1.122
$R1[I > 2\sigma(I)]$	0.0478	0.0388
$wR2$[all data]	0.1083	0.0932
$\Delta\rho_{max}$, $\Delta\rho_{min}$ (e Å^{-3})	0.503, -0.298	0.792, -0.263
Weight. scheme (A, B)	0.0522, 0.30	0.0424, 2.26

D.[20] The isotropic Heisenberg exchange term used in the Hamiltonian is of the form $-2J\hat{S}_1\hat{S}_2$.

3.2.3. X-ray crystallography

X-ray data were collected for **1** and **2** on a Bruker SMART APEX CCD X-ray diffractometer, using graphite-monochromated Mo-Kα radiation (λ = 0.71073 Å). Data were reduced using SAINTPLUS[21] and a multi-scan absorption correction was applied using SADABS.[22] The structure was solved using SHELXS-97 and full matrix least squares refinement against F^2 was carried out using SHELXL-97.[23] All ring hydrogen atoms were assigned on the basis of geometrical considerations and were allowed to ride upon the respective carbon atoms with fixed U_{iso} values: $1.2U_{eq}$ of the parent atom (ring hydrogen atoms), $1.5U_{eq}$ for methyl and water hydrogen atoms. In **2**, one of the two lattice water molecules is disordered about the crystallographic mirror plane. Crystallographic data and structure refinement parameters are presented in Table 3.1.

3.3. Results and discussion

3.3.1. Synthesis

Both compounds were prepared by a similar procedure, except that compound **1** crystallized at 5º C, while **2** was obtained at about 25º C. Attempts to obtain other polymorphs of these complexes were not successful. Though in both cases the Schiff base was generated *in situ*, pure methanolic medium was used for the preparation of **1** while in the case of **2**, the crystals were obtained in a largely

aqueous medium. A previous preparation[3] using an acphenH_2 solution and Mn^{II} perchlorate hydrate resulted in the isolation of the mononuclear complex Mn(acphen)(H_2O)(NCS) as anhydrous crystals.

3.3.2. Crystal structure of [Mn(acphen)NCS]$_2$ (1)

Each unit of the phenoxo bridged dimer is made up of a tetradentate acphen ligand binding the Mn(III) ion in equatorial mode and an N-bonded terminal thiocyanato ion occupying the axial position (Figure 3.1). The structure has a crystallographic inversion centre at the mid point of the dimeric core. The Mn···O_p (where O_p is the oxygen atom of the phenoxo-bridge) bond distance is 2.411(2) Å and the bridge angle, Mn–O_p···Mn' is 102.14(7)º, both within the range of Type-1 out-of-plane dimers.[9] The Mn···Mn' distance is 3.374 Å. The basal atoms are approximately coplanar with deviations of 0.10 Å from the mean plane. The central Mn atom is displaced by 0.14 Å towards the thiocyanato ligand. The two halves of the acphen ligand, excluding the methylene and methyl groups are each nearly planar (rms deviations = 0.05, 0.07 Å) with an interplanar angle of 17.5º. The two halves of the ligand are unsymmetrically disposed about the basal coordination plane with interplanar angles of 12.7 and 29.0º. No short inter-dimer contacts are observed, the nearest intermolecular Mn···Mn' distance being 7.913 Å. The plane defining the $Mn_2(O_p)_2$ bridge makes an angle of 88.9º with the basal coordination plane, MnN_2O_2. The overall coordination geometry of each Mn(III) ion is distorted octahedral with the Jahn-Teller elongation along the SCN-Mn···O_p axis. Selected bond distances and angles are given in Table 3.2.

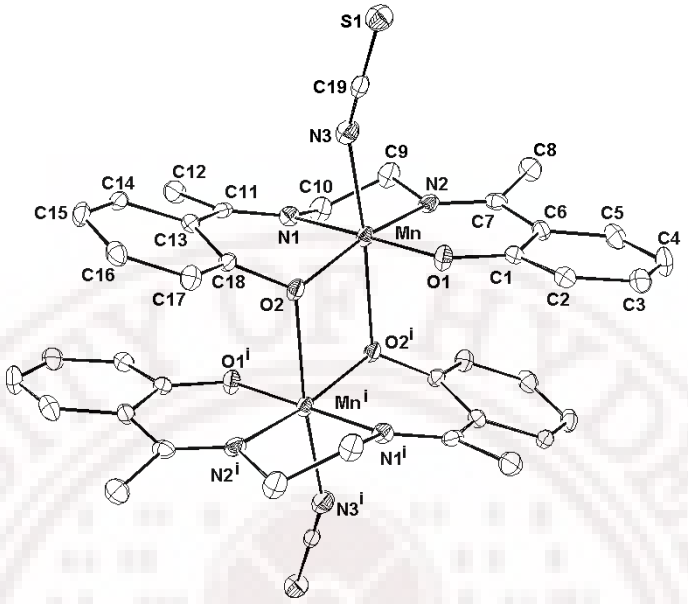

Figure 3.1 ORTEP view of the $[Mn(acphen)NCS]_2$ (**1**) with atom labeling. Atoms are shown as 30% thermal ellipsoids. Hydrogen atoms are omitted for clarity. (i) *–x*, *–y*, *–z*+1

Table 3.2 Selected bond lengths [Å] and angles [°] for $[Mn(acphen)NCS]_2$ (**1)**

Mn-O1	1.8572(16)	Mn-N1	1.992(2)	Mn-N3	2.169(2)
Mn-O2	1.9070(16)	Mn-N2	1.998(2)	Mn-O2#1	2.4109(17)
N3-C19	1.165(3)	C19-S1	1.631(3)		
O1-Mn-N1	91.58(8)	N1-Mn-N2	84.83(8)	O2-Mn-O2#1	77.86(7)
O1-Mn-N2	175.77(8)	N1-Mn-N3	98.24(8)	N1-Mn-O2#1	87.96(7)
O1-Mn-N3	91.41(8)	N2-Mn-N3	91.32(8)	O1-Mn-O2#1	89.99(7)
O1-Mn-O2	94.34(7)	O2-Mn-N1	164.61(8)	N2-Mn-O2#1	87.65(7)
O2-Mn-N3	95.80(8)	O2-Mn-N2	88.59(7)	N3-Mn-O2#1	173.60(7)
Mn-N3-C19	152.5(2)	N3-Mn-S1	179.2(2)	Mn-O2-Mn#1	102.14(7)

#1 *-x*, *-y*, *-z*+1

3.3.3. Structure of $[Mn(acphpn)(H_2O)NCS]\cdot 2H_2O$ (2)

The structure is entirely different from the previous one, the formation of dimer/polymer being prevented by the coordinated water molecule. As shown in Figure 3.2, the Mn(III) coordination has a distorted octahedral geometry. The tetradentate acphpn ligand chelates the Mn atom in the equatorial mode, the apical positions being occupied by an N-bonded terminal thiocyanato and a water molecule. The coordination of the thiocyanato ion is nearly linear, the Mn–N–C angle being 177.7º. The equatorial donors N1, N1', O1 and O1' are exactly in a plane and the manganese atom is displaced by 0.065 Å towards the coordinated water molecule. However, the ligand as a whole is grossly non-planar, even after excluding the methylene groups, the angle between the mean planes of the two halves being 71.6º. The two halves are thereby greatly bent towards the water ligand and away from the thiocyanato. The non-methylated ligand is known to form two polymorphs[2b], a phenoxo bridged dimer in which the above mentioned inter-planar angle is 10º and a helical chain in which the angle is 37º. Selected bond distances and angles are given in Table 3.3. Two solvent water molecules are present in the lattice, which are hydrogen bonded to the complex molecule to build a one dimensional chain as shown in Figure 3.3. The hydrogen bonding parameters are presented in Table 3.4.

There are some features worth noting in the crystal structure of **2**. Regarding the molecular structure, the Mn–N–C–S atoms are arranged in a closely linear mode, at variance with most other structures where the terminal thiocyanato and Mn(III) are bonded in a bent mode.[2b,3,9,12b,24-29] A notable exception is a five coordinate complex

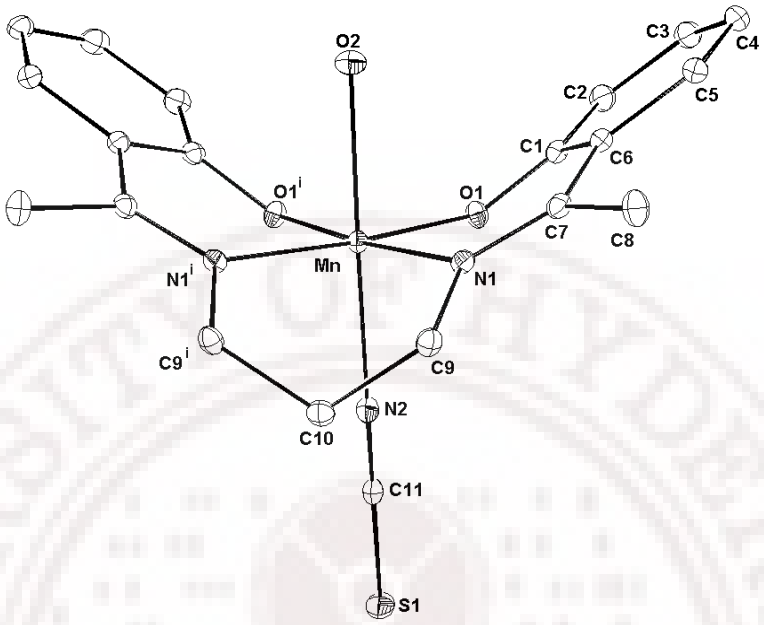

Figure 3.2 ORTEP view of [Mn(acphpn)(H_2O)(NCS)].2H_2O (**2**) with atom labelling. Atoms are shown as 30% thermal ellipsoids. All hydrogen atoms and lattice water molecules are omitted. Symmetry: (i) *x*, *–y*+1/2, *z*.

Table 3.3 Selected bond lengths [Å] and angles [°] for [Mn(acphpn)(H_2O)(NCS)].2H_2O (**2**)

Mn-O1	1.8869(12)	Mn-N1	2.0402(14)	Mn-O1#1	1.8869(12)
Mn-O2	2.2349(18)	Mn-N2	2.247(2)	Mn-N1#1	2.0402(14)
N2-C11	1.152(3)	C11-S1	1.647(3)		
O1-Mn-N1	87.97(5)	N1-Mn-N2	96.62(5)	O1#1-Mn-O1	89.40(7)
O1-Mn-O2	89.01(5)	O2-Mn-N1	87.23(5)	O1#1-Mn-N1	175.44(6)
O1-Mn-N2	86.95(5)	O2-Mn-N2	174.31(7)	N1#1-Mn-N1	94.41(8)
Mn-N2-C11	177.7(2)	N2-C11-S1	179.4(2)	#1 *x, –y* +1/2, *z*	

where the thiocyanato and Mn are located on a crystallographic two fold axis, and hence strictly linear.[30] Alike in that structure, the linear coordination results in a shorter N–C bond for **2** compared to **1**. The C–N stretching frequencies seen in the IR spectra are also significantly different: 2054 cm^{-1} in **1** and 2085 cm^{-1} in **2**. These observations are in line with the expectation of a bond order higher than two for a linearly coordinated thiocyanato. Concerning the three water molecules, the coordinated one is situated fully on the mirror plane while one of the lattice water molecules is bisected by the mirror plane and the other one is disordered about this plane. These features related to the mirror symmetry element can be rationalized by the coordination and hydrogen bonding requirements. While the bisecting mode is unsuitable for a coordinated water molecule, it creates no problem for a lattice water molecule. The fact that these two water molecules attain saturation with regard to hydrogen bonding (Figure 3.3) seems to "protect" them from being disordered. The second water molecule has only one acceptor so that the entropy driven disorder about the mirror plane operates for it.

Table 3.4 Hydrogen bonding parameters for [Mn(acphpn)(H_2O)(NCS)].2H_2O (**2**)

D-H···A	D-H (Å)	H···A (Å)	D···A (Å)	D-H···A (º)
O2-H2A···O3	0.826	1.950	2.775	175.12
O2-H2B···O4#1	0.716	2.059	2.689	147.22
O3-H3B···O1#2	0.871	2.059	2.812	144.19
O4-H4B···O3#3	0.893	2.114	2.912	148.42

#1 *x*, –*y*+1/2, *z*; #2 *x*+1/2, *y*, –*z*+1/2; #3 *x*+1, *y*, *z*

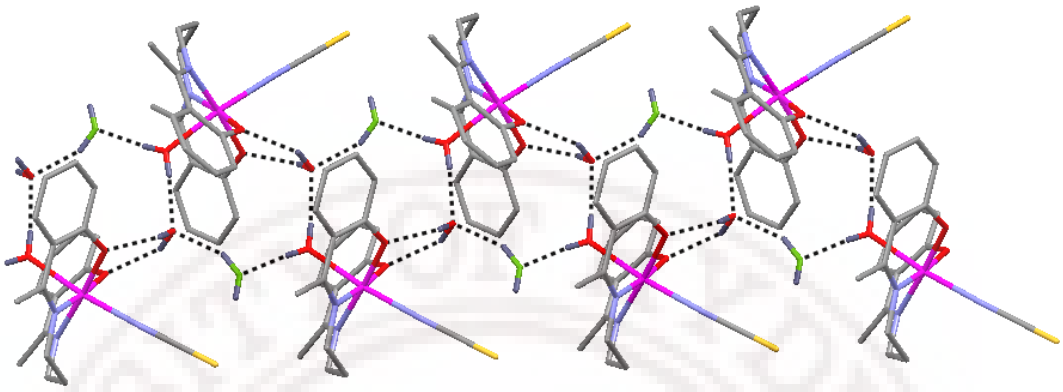

Figure 3.3 One-dimensional hydrogen bonded chains in complex **2**. The lattice water molecule with one free hydrogen atom is disordered about the crystallographic mirror plane. For the purpose of illustration it has been moved to the mirror plane.

3.3.4. Spectral Studies

3.3.4a. FTIR Spectra

The IR spectra of compound **1** and **2** exhibit strong absorption in the range of 2040-2090 cm^{-1}, which is attributed to the asymmetric stretching vibration of N-bonded thiocyante group and the strong absorption at 1590-1645 cm^{-1}, which is assignable to the (-C=N) stretching vibration of Schiff-base. Compound **2** exhibits broad absorption bands at 3344, 3200 cm^{-1}, which is attributed stretching vibration (O-H) of water molecules. All these absorptions are with in the reported range.[31]

3.3.4b. Electronic Spectra

The solution spectra of the compounds **1** and **2** were measured in methanol (Figure 3.4). The low intensity absorption bands in the range 16.67, 425(sh) for

complex **1** and 16.67, 551(sh) for complex **2** ($\bar{\nu}_{max}$ /10^3cm^{-1}, ε_{max}/cm^{-1}M^{-1}) respectively, which are assigned to d-d transition. The high intensity absorption bands in the range 17.62, 522; 25.86, 5589; 35.64, 17721 for complex **1** and 17.62, 588; 26.91, 8162; 35.97, 17292 for complex **2** ($\bar{\nu}_{max}$ /10^3cm^{-1}, ε_{max}/cm^{-1}M^{-1}) respectively, which are assigned to intraligand π-π* transitions in the complexes, the low intensity d-d transitions were masked in this range.

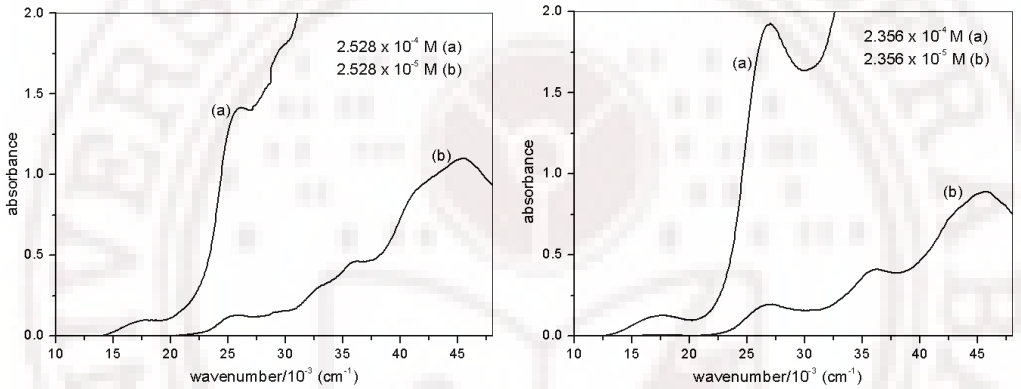

(1) **(2)**

Figure 3.4 Electronic absorption spectra Solution spectra of complex **1** and **2** in methanol.

3.4. Magnetic Properties

The temperature-dependence of the magnetic susceptibility χ_m, of **1** and **2** was measured in the temperature range 1.98-300 K (Figures 3.5 and 3.6). The $\chi_m T$ value of **1** per magnetic ion is 2.97 cm^3 mol^{-1} K at 300 K (close to the expected spin-only value, 3.00 cm^3 mol^{-1} K per Mn(III)). While decreasing the temperature, there is no significant change up to about 80 K, from where $\chi_m T$ decreased to 1.30 cm^3 mol^{-1} K per Mn(III) at 5.8 K and 0.414 cm^3 mol^{-1} K per Mn(III) at 2.0 K. The decrease is characteristic of an antiferromagnetic exchange interaction between the two high-

spin Mn(III) ions. The best fit to the dimer equation[18a] yielded the parameters values $J = -0.79(1)$ cm^{-1}, $zJ' = -0.017(1)$ cm^{-1}, $g = 2.00$, L.S. Error = 0.000470. The weakness of the inter-dimer interaction (small magnitude of zJ'), which is in agreement with the absence of significant inter-dimer contacts in the crystal, suggests operation of single ion zero-field splitting. Exact diagonalisation of the spin Hamiltonian including axial Zeeman and zfs terms in addition to isotropic exchange led to the following best fit parameters: $J = -0.7(1)$ cm^{-1}, $D = -0.6(1)$ cm^{-1}, $g = 2.017(5)$, L.S. Error = 0.00013.

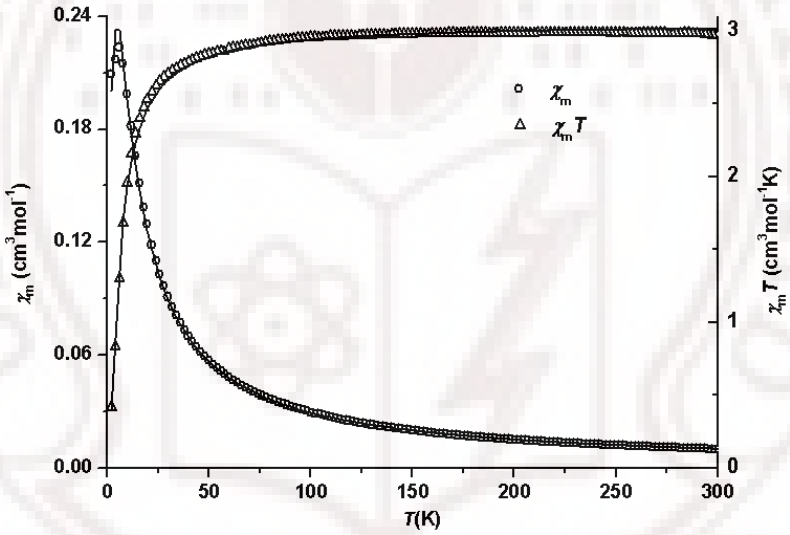

Figure 3.5 Temperature variation of magnetic susceptibility (per magnetic ion) for compound **1**. The solid lines result from a least-squares fit to the data of the theoretical values calculated through exact diagonalisation of the spin Hamiltonian including axial Zeeman, zfs and isotropic exchange terms as explained in the text.

The fitting is unique, and in particular, a positive value for *D* leads to divergence. This is satisfying because, a Jahn-Teller elongated Mn(III) complex is expected to have a small negative *D*.[32] Finally, the geometry of the bridge (Mn–O, 1.91, 2.41Å; Mn–O–Mn, 102.1º) is in the range usually reported[9] for phenoxo-bridged complexes characterized by antiferromagnetic interactions.

The $\chi_m T$ value of **2** at 300K is 3.38 $cm^3\ mol^{-1}$ K, slightly higher than the spin-only value of 3.00 $cm^3\ mol^{-1}$ K per Mn^{III}. With decreasing temperature, $\chi_m T$ also decreased and reached a value of 1.27 $cm^3\ mol^{-1}$ K per Mn(III) at 1.98 K, indicating weak intra-chain antiferromagnetic interactions. The data were fitted to both the Curie-Weiss equation[18a] as well as the Heisenberg chain equation[18b] with the following results: Curie-Weiss: g = 2.12(fixed), θ = – 3.76 (5) K, L.S. Error = 0.00623; chain, g = 2.12(fixed), J = – 7.82(2) cm^{-1}, θ = 1.18(2) K, L.S. Error = 0.00008. A comment on the validity of the above parameters is in order. A *g*-value significantly greater than 2 and a ferromagnetic interchain coupling as implied by the positive θ are difficult to explain. Moreover, it is found that J and θ are strongly correlated. If g is fixed at 2.0, it is possible to get equally good fit for two sets of parameters: J = – 5.59(9) cm^{-1}, θ = 1.07(2) K, L.S. Error = 0.003; J = +0.7(1) cm^{-1}, θ = – 4.2(2) K, L.S. Error = 0.004. If θ is not included, the best fit is obtained with J = – 2.40 cm^{-1}, g = 1.95 with a relatively high L.S. Error of 0.01. Omitting θ but including the interchain interactions through the mean-field leads to divergence. Only the Curie-Weiss fit is included in Fig. 5. The only valid conclusion that can be drawn from the data is that there is weak antiferromagnetic interaction in the crystals of this mononuclear Mn(III) complex characterized by *J*-value of about – 2 cm^{-1}.

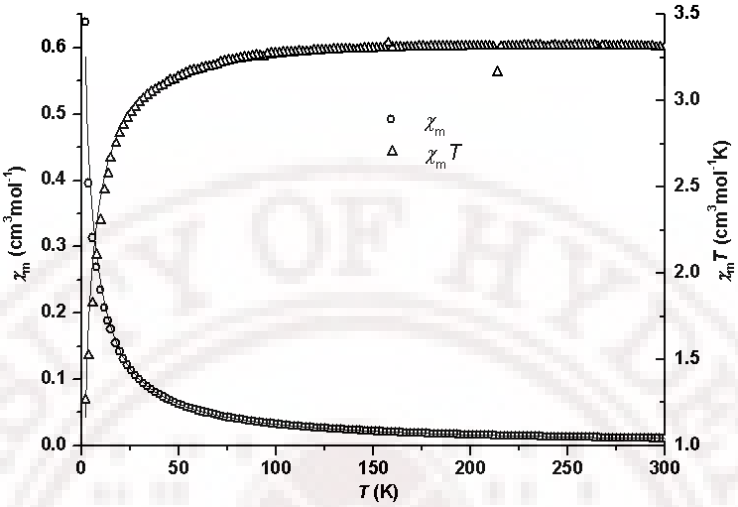

Figure 3.6 Temperature variation of magnetic susceptibility (per magnetic ion) for compound **2**. The solid line results from a least-squares fit to the data of the theoretical values calculated with the Curie-Weiss equation.

It is instructive to compare the above result for compound **2** with the magnetic properties of the homologous complex [Mn(acphen)(H_2O)NCS], the crystals of which contain no lattice water.[3] However, it is first necessary to analyze the possible exchange pathways in **2,** all of which involve hydrogen bonding among coordinated water (CW), lattice water (LW) and coordinated Schiff base oxygen (SBO) atoms. If for a moment the disordered lattice water (the one with a free hydrogen atom in Figure 3.3) is ignored, one gets a zig-zag chain in which the adjacent Mn(III) centers are connected by a 5-atom CW–LW–SBO bridge. The second lattice water molecule, though disordered, introduces two additional bridges in the 1-dimensional system: CW–LW–LW–SBO and CW–LW–LW–CW, both involving seven atoms. If one considers the topology of these bridges with reference

to the Mn(III) centers, two types can be recognized: Type-I, z – (x, y), which connects a ligand in the axial position (water, in this compound) to one or more ligands in the equatorial plane (the two Schiff base oxygen atoms) and Type-II, z – z, in which two axial ligands are inter-connected. The magnetic orbitals for a d^4 ion in an axially elongated octahedral complex are d_{xy}, d_{xz}, d_{yz}, and d_{z2}. Super-exchange involving these orbitals will be weak because, the first three are essentially π-bonding while the last one is σ-bonding but its overlap with the axial ligand is small. Nevertheless, the relative strengths of these pathways can be inferred by comparing with the above mentioned homologous complex of acphen. The crystal structure of this complex[3] is also built from 1-dimensional hydrogen bonded chains generating just one CW–SBO (3-atom, Type-I) bridge, there being no lattice water in the crystals of this compound. Remarkably, the acphen complex has a constant μ_{eff} value of 4.96 B.M. in the temperature range 6-300 K indicating that there is no intermolecular magnetic interaction. It is therefore reasonable to conclude that the 7-atom Type-II bridge is responsible for the weak antiferromagnetic coupling observed in compound **2** (Figure 3.7).

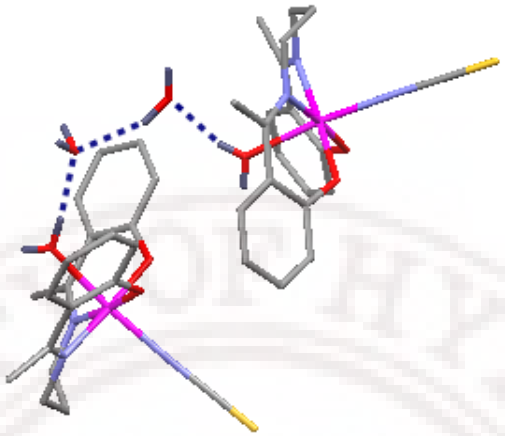

Figure 3.7 Antiferromagnetic exhange pathway via lattice water in compound **2**.

3.5. Conclusions

The weak antiferromagnetic interaction in $[Mn(acphen)NCS]_2$ and $[Mn(acphpn)(H_2O)NCS]\cdot 2H_2O$ has different origins. In the case of the acphen complex, two phenoxo bridges are involved. According to the classification given above, these are single atom Type-I bridges. For the acphpn complex, the exchange pathway is made up of multi atom bridges involving hydrogen bonded lattice water, the dominant contribution being attributed to a 7-atom Type-II bridge. The similar magnitudes of the Heisenberg exchange parameter (J) for these two structurally very different systems do not mean that the pathways are equally efficient. The small negative value of J for the phenoxo dimer may result from near cancellation of moderately strong ferro and antiferromagnetic contributions from the four different magnetic orbitals on each Mn(III) centre. The most significant result from the present study arises from comparison of the acphpn aquo complex with the previously

studied similar mononuclear Mn(III) complex of acphen, the only important difference being the absence of lattice water in its crystals. It is shown that hydrogen bonding through lattice water provides a pathway for exchange in the present complex while the previous compound, though consisting of hydrogen bonded chains, has no significant magnetic interaction. A definitive characterization of the role of lattice water in transmitting magnetic coupling across multi-atom bridges has been previously reported for a Cu(II) complex.[33] Measurement and understanding of the role of solvent molecules in transmitting magnetic information across long distances is important in the context of, among other things, bio-inorganic chemistry and quantum computing.

3.6. References

1. For an early study of Mn(III) tetradentate Schiff base crystals, See: Joseph, A. B.; Martin L. K.; Myoung, S. L.; Dimitri, P. K.; William, E. H.; Vincent L. P. *Inorg. Chem.* **1989**, *28*, 180.
2. (a) Reddy, K. R.; Rajasekharan, M. V.; Tuchagues, J.-P. *Inorg. Chem.* **1998**, *37*, 5978. (b) Sailaja, S.; Rajasekharan, M. V.; Hureau, C.; Riviere, E.; Cano, J.; Girerd J.-J. *Inorg. Chem*. **2003**, *42*, 180.
3. Chakraborty, J.; Brajagopal, S.; Pilet, G.; Mitra, S. *Struct. Chem.* **2006**, *17*, 585.
4. Lecren, L.; Wernsdorfer, W.; Li, Y. -G.;Vindigni, A.; Miyasaka, H.; Clerac, R. *J. Am. Chem. Soc*. **2007**, *129*, 5045.

5. Lu, Z.; Yuan, M.; Pan, F.; Gao, S.; Zhang, D.; Zhu, D. *Inorg. Chem.* **2006**, *45*, 3538 (and references therein).

6. Karmakar, R.; Choudhury, C. R.; Bravic, G.; Sutter, J.-P.; Mitra, S. *Polyhedron* **2004**, *23*, 949.

7. Shyu, H.; Wei, H.; Wang, Y. *Inorg. Chim. Acta* **1999**, *290*, 8.

8. (a) Mabad, B.; Luneau, D.; Theil, S.; Dahan, F.; Savariault, J. M.; Tuchagues, J. - P. *J. Inorg. Biochem.* **1991**, *43*, 373. (b) Kennedy, B. J.; Murray, K. S. *Inorg. Chem*. **1985**, *24*, 1552.

9. Miyasaka, H.; Clerac, R.; Ishii, T.; Chang, H.; Kitagawa, S.; Yamashita, M. *J. Chem. Soc., Dalton Trans*. **2002**, 1528.

10. Bermejo, M. R.; Castineiras, A.; Garcia-Montergudo, J. C.; Rey, M.; Sousa, A.; Watkinson, M.; McAuliffe, C. A.; Pritchard, R. G.; Beddose, R. I. *J. Chem, Soc., Dalton Trans.* **1996**. 2935.

11. Matsumoto, N.; Zhong, Z.; Okawa, H.; Kida, S. *Inorg. Chim. Acta* **1989**, *160*, 153.

12. (a) Matsumoto, N.; Takemoto, N.; Ohyosi, A.; Okawa, H. *Bull. Chem. Soc. Jpn.* **1988**, *61*, 2984. (b) Mikuriya, M.; Yamato, Y.; Tokii, T. *Bull. Chem. Soc. Jpn.* **1992**, *65*, 1466.

13. Garcia-Deibe, A.; Sousa, A.; Bermejo M, R.; MacRory, P. P.; McAuliffe, C. A.; Pritchard, R. G.; Helliwell, M. *J. Chem. Soc., Chem. Commun.* **1991**, 728.

14. Miyasaka, H.; Sugimoto, K.; Sugiura, K.; Ishii, T.; Yamashita, M. *Mol. Cryst. Liq. Cryst.* **2002**, *379,* 197.

15. Miyasaka, H.; Mizushima, K.; Furukawa, S.; Sugiura, K.; Ishii, T.; Yamashita, M. *Mol. Cryst. Liq. Cryst.* **2002**, *379*, 171.

16. Sato, Y.; Miyasaka, H.; Matsumoto, N.; Okawa, H. *Inorg. Chim. Acta* **1996**, *247*, 57.

17. Miyasaka, H.; Saitoh, A.; Abe, S. *Coord. Chem. Rev.* **2007**, *251*, 2622.

18. Chandramouli, G. V. R.; Balagopalakrishna, C.; Rajasekharan, M. V.; Manoharan, P. T. *Comput. Chem.* **1996**, *20*, 353.

19. (a) O'Connor, C. J. *Prog. Inorg. Chem.* **1982***, 29*, 203. (b) Koenig, E.; Desai, V. P.; Kanallakopulos, B; Klenze, R. *Chem. Phys.* **1980**, *54*, 109.

20. Garge, P.; Chikate, R.; Padhye, S.; Savariault, J.-M.; de Loth, P.; Tuchagues, J.-P. *Inorg. Chem*. **1990**, *29*, 3315.

21. *SAINTPLUS*, Bruker AXS Inc., Madison, Wisconsin, USA 2003.

22. Sheldrick, G. M. *SADABS, Program for empirical absorption correction*, University of Gottingen, Gottingen, Germany 1996.

23. Sheldrick, G. M. *SHELX-97*, *Programs for crystal structure analysis*, University of Gottingen, Gottingen, Germany 1997.

24. Nastase, S.; Tuna, F.; Maxim, C.; Muryn, C. A.; Avarvari, N.; Winpenny, R. E. P.; Andruh, M. *Cryst. Growth Des*. **2007**, *7*, 1825.

25. Biswas, S.; Mitra, k.; Schwalbe, C.H.; Lucas, C. R.; Chattopadhyay, S. K.; Adhikary. B. *Inorg. Chim. Acta* **2005**, *358*, 2473.

26. Li, H.; Zhong, Z. J.; Duan, C. -Y.; You, X. -Z.; Mak, T. C. W.; Wu, B. *J. Coord. Chem.* **1997**, *41*, 183.

27. Yun-Long, F.; Shi-Xiong, L. *Chin. J. Struct. Chem.* **1996**, *15*, 47.

28. (a) Feng, Y. -L.; Liu, S. -X. *J. Coord. Chem.* **1998**, *44*, 81. (b) Shou-Bin, W.; Kun, T.; Bao-Hua, Y.; Sheng, L. *Acta Crystallogr.* **2008**, *E64*, m543.

29. Bertoncello, K.; Fallon, G. D.; Murray, K. S.; Tiekink, E. R. T. *Inorg. Chem.* **1991**, *30*, 3562.

30. Weiss, M. C.; Goedken, V. L. *Inorg. Chem.* **1979**, *18*, 274.

31. Nakamoto, K. *Infrared and Raman Spectra of Inorganic and coordination Compounds*; 3 ed.; John Wiley & Sons, Inc.: New York, 1997, pp 270.

32. (a) Kennedy, B. J.; Murray, K. S. *Inorg. Chem*. **1985**, *24*, 1557. (b)Whittaker, J. W.; Whittaker, M. M. *J. Am. Chem. Soc*. **1991**, *113*, 5528. (c) Zhang, Z.-Y.; Brouca-Cabarrecq, C.; Hemmert, C.; Dahan, F.; Tuchagues, J.-P. *J. Chem. Soc. Dalton Trans*. **1995**, 1453.

33. Balagopalakrishna, C.; Rajasekharan, M. V. *Phys. Rev. B* **1990**, *42*, 7794.